

3-30-2022

Vacuum UV (VUV) Photo-Oxidation of Polyethersulfone (PES)

Sarah Oakes

Rochester Institute of Technology

Ryan Keeley

Rochester Institute of Technology

Hunter Heineman

Rochester Institute of Technology

Tom Allston

Rochester Institute of Technology

Joel Shertok

Rochester Institute of Technology

See next page for additional authors

Follow this and additional works at: <https://repository.rit.edu/article>

Recommended Citation

Oakes, S.; Keeley, R.; Heineman, H.; Allston, T.; Shertok, J.; Mehan, M.; Thompson, G.K.; Takacs, G.A.
Vacuum UV (VUV) PhotoOxidation of Polyethersulfone (PES). *Technologies* 2022, 10, 49. <https://doi.org/10.3390/technologies10020049>


This Article is brought to you for free and open access by the RIT Libraries. For more information, please contact repository@rit.edu.

Authors

Sarah Oakes, Ryan Keeley, Hunter Heineman, Tom Allston, Joel Shertok, Michael Mehan, Gregory K. Thompson, and Gerald A. Takacs

Article

Vacuum UV (VUV) Photo-Oxidation of Polyethersulfone (PES)

Sarah Oakes ¹, Ryan Keeley ¹, Hunter Heineman ¹, Tom Allston ¹, Joel Shertok ¹, Michael Mehan ² , Gregory K. Thompson ² and Gerald A. Takacs ^{1,*}

¹ Plasma Laboratory, School of Chemistry and Materials Science, Rochester Institute of Technology, Rochester, NY 14623, USA; sao3140@g.rit.edu (S.O.); rpk8784@g.rit.edu (R.K.); hdh3020@g.rit.edu (H.H.); tdasch@rit.edu (T.A.); jshertok@yahoo.com (J.S.)

² Xerox Analytical Services, Xerox Corporation, Webster, NY 14580, USA; Michael.Mehan@xerox.com (M.M.); Gregory.Thompson@xerox.com (G.K.T.)

* Correspondence: gatsch@rit.edu; Tel.: +1-585-475-2047

Abstract: International need for water quality is placing a high demand on separation technology to develop advanced oxidative processes for polyethersulfone (PES) membranes to help improve water purification. Therefore, VUV photo-oxidation with a low pressure Ar plasma was studied to improve the hydrophilicity of PES by flowing oxygen over the surface during treatment. X-ray photoelectron spectroscopy (XPS) detected a decrease in the C at% (4.4 ± 1.7 at%), increase in O at% (3.7 ± 1.0 at%), and a constant S at% (5.4 ± 0.2 at%). Curve fitting of the XPS spectra showed a decrease in sp^2 C-C aromatic group bonding, and an increase in C-O, C-S, O=C-OH, sulphonate ($-SO_3$) and sulphate ($-SO_4$) functional groups with treatment time. The water contact angle decreased from 71.9° for untreated PES down to a saturation level of 41.9° with treatment. Since scanning electron microscopy (SEM) showed no major changes in surface roughness, the increase in hydrophilicity was mainly due to oxidation of the surface. Washing the VUV photo-oxidized PES samples with water or ethanol increased the water contact angle saturation level up to 66° indicating the formation of a weak boundary layer.

Keywords: surface modification; polyethersulfone (PES); VUV photo-oxidation; hydrophilicity; XPS; water contact angle; SEM



Citation: Oakes, S.; Keeley, R.; Heineman, H.; Allston, T.; Shertok, J.; Mehan, M.; Thompson, G.K.; Takacs, G.A. Vacuum UV (VUV) Photo-Oxidation of Polyethersulfone (PES). *Technologies* **2022**, *10*, 49. <https://doi.org/10.3390/technologies10020049>

Academic Editor: Niko Münzenrieder

Received: 18 February 2022

Accepted: 25 March 2022

Published: 30 March 2022

Publisher's Note: MDPI stays neutral with regard to jurisdictional claims in published maps and institutional affiliations.



Copyright: © 2022 by the authors. Licensee MDPI, Basel, Switzerland. This article is an open access article distributed under the terms and conditions of the Creative Commons Attribution (CC BY) license (<https://creativecommons.org/licenses/by/4.0/>).

1. Introduction

The international need for water quality is placing a high demand on separation technology. Different membrane filtrations are required depending on the increasing particle sizes of the solutes, such as hydrated ions, proteins, viruses, bacteria, algae, and colloids (requiring, e.g., reverse osmosis, nanofiltration, ultrafiltration, microfiltration, and conventional filtration). Solutes collecting on the surface and within the pores of the membrane cause a decreasing flux of water, resulting in higher maintenance and operating expenses. Therefore, a variety of surface modification techniques, such as blending, grafting, chemical treatment, plasma treatment, UV irradiation, gamma rays, and electron beams, are used to influence the surface wettability (i.e., hydrophilicity, and roughness to make the surface more attractive to water and repulsive to the organic waste) [1–6]. Advanced oxidative processes need to be developed to help improve water purification.

Polyethersulfone (PES) (Figure 1) is a membrane often used in the operation of water cleaning devices due to its superior thermal, mechanical, and chemical properties which assist in the construction of different surfaces and pore sizes [1–6]. In this study, vacuum UV (VUV) photo-oxidation [7] with a low pressure Ar plasma was used to improve the hydrophilicity properties of PES by flowing oxygen over the surface of PES during treatment. The plasma excites Ar atoms which emit VUV photons having wavelengths of 104.8 and 106.7 nm due to $^3P_1 \rightarrow ^1S_0$ and $^3P_2 \rightarrow ^1S_0$ transitions, respectively [8]. The high VUV photo-absorption coefficients (10^4 – 10^5 cm^{-1}) of polymers results in penetration depths not

exceeding a few hundred nms, hence producing surface modification without altering the bulk properties [7].

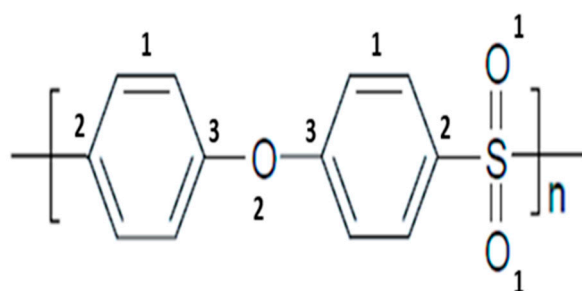


Figure 1. Structure of PES illustrating three different C bondings: (1) C=C, (2) C-S, and (3) C-O and two O bondings: (1) O=S, and (2) O-C.

2. Materials and Methods

2.1. Materials

PES film (0.125 mm thick), purchased from Goodfellow Corp. (Coraopolis, PA, USA) (catalog no. 494-219-10), was cleaned with Koptec 200 proof ethanol (DLI, King of Prussia, PA, USA) in an ultrasonic bath for 20 min and then stored in a closed petri dish for at least 24 h.

2.2. VUV Photo-Oxidation

The experimental setup was similar to that used in the VUV photo-oxidation of other polymers [7] such as polystyrene [9] and polybenzimidazole [10]. VUV radiation was generated from a low-pressure argon microwave (MW) plasma, having an absorbed power of 26–34 W, to modify the surface of PES located 23.8 cm downstream from the discharge. At this distance, charged particles and metastables, due to deactivation and recombination processes involving homogeneous and heterogeneous collisions in transit to the substrate, contribute negligibly and thus the interaction of VUV photons with the substrate is maximized [11,12]. Oxygen was introduced into the vacuum system about 3 cm above the sample. The argon and oxygen flow rates were 50 and 10 sccm, respectively. The reaction chamber pressure was maintained at 66–80 Pa and the samples were treated at various times up to 200 min.

Coupling the photoabsorption cross sections of oxygen molecules at these wavelengths together with the oxygen number density and pathlength through the oxygen, more than 93% of the VUV radiation from the Ar MW discharge is transmitted through the oxygen to help modify the PES surface. Photoabsorption by oxygen in the VUV region of the electromagnetic spectrum ([13], pp 206-207) results in the production of ground state, 3P , and electronically excited, 1D and 1S , oxygen atoms ([14], pp. 179) which assist in the surface modification.

2.3. X-ray Photoelectron Spectroscopy (XPS)

As reported in [9,10], XPS analysis was carried out using Physical Electronics Versaprobe II 5000 equipment which examined the top 2–5 nm of a sample's surface using a take-off angle of 45° . The quantitative analyses are accurate within 5% for major constituents and 10% for minor constituents.

The chemical state analysis of the C 1s, O 1s, and S 2p spectra were achieved by normalized the peak intensities at the main peaks, and curve-fitting was carried out comparing spectra with a cleaned and untreated PES sample. The control spectrum was subtracted from the treated spectrum and the remainder spectrum was curve-fitted to determine the number of peaks, their binding energies, and peak widths resulting from treatment. The peaks from the remainder spectrum were used to curve-fit the total treated spectrum. Weak energy loss peaks were then added to the curve-fitting to achieve a good

chi square fit and a materials balance was conducted to test if the results of the curve-fitting agreed with the quantitative analyses results.

2.4. Contact Angle (CA) Goniometry

As described in ref. [9], water contact angles were obtained using a Ramé-Hart model 500 Standard Contact Angle Goniometer. The samples were placed on double-sided tape to keep the surface flat and a micropipette was used to deposit a 10 μ L deionized water droplet on the surface. As soon as the water droplet was placed on the film, a picture was captured by the DROPimage contact angle (CA) program. The standard deviation of the measurements was about $\pm 2.5^\circ$.

2.5. Scanning Electron Microscopy (SEM)

Surface topography was determined using a JEOL JSM-7200FLV FESEM at 5 kV accelerating voltage with an invisible film of platinum sputter-coated on the samples to eliminate electrostatic charging.

3. Results

3.1. Quantitative XPS and Water Contact Angle

The XPS quantitative analysis for five untreated samples gave atomic percentages for C, S, and O of 73.4 ± 0.9 , 5.4 ± 0.2 , and 21.2 ± 0.9 at% in good agreement with the values from the molecular structure (Figure 1): 75, 6.2, and 18.8 at%, respectively. Within experimental error, the treated samples gave constant results after 60 min of treatment showing the C at% decreased by 4.4 ± 1.7 at%, the O at% increased by 3.7 ± 1.0 at%, while the S at% remained approximately unchanged (5.4 ± 0.2 S at%).

Figure 2 displays an example of the water contact angle changes with treatment time.

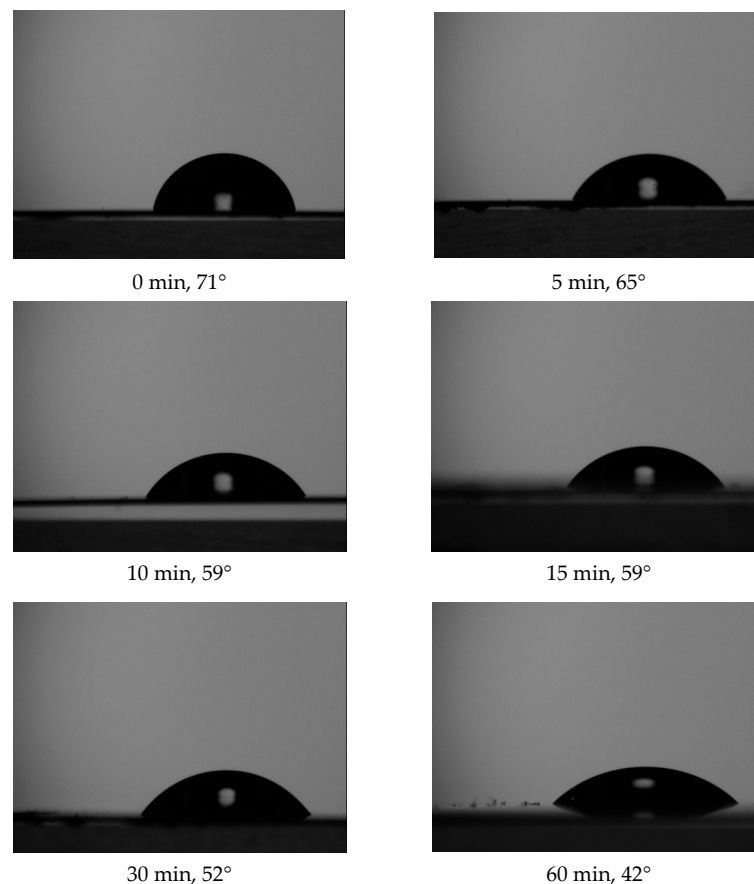


Figure 2. Water contact angle measurements in degrees after PES was treated with VUV photo-oxidation for 0, 5, 10, 15, 30, and 60 min.

Figure 3 shows the average at% O results for five sets of samples treated for 5, 10, 15, 30, and 60 min together with the average water contact angle measurements decreasing from 71.9° down to 41.9° after 60 min of treatment time.

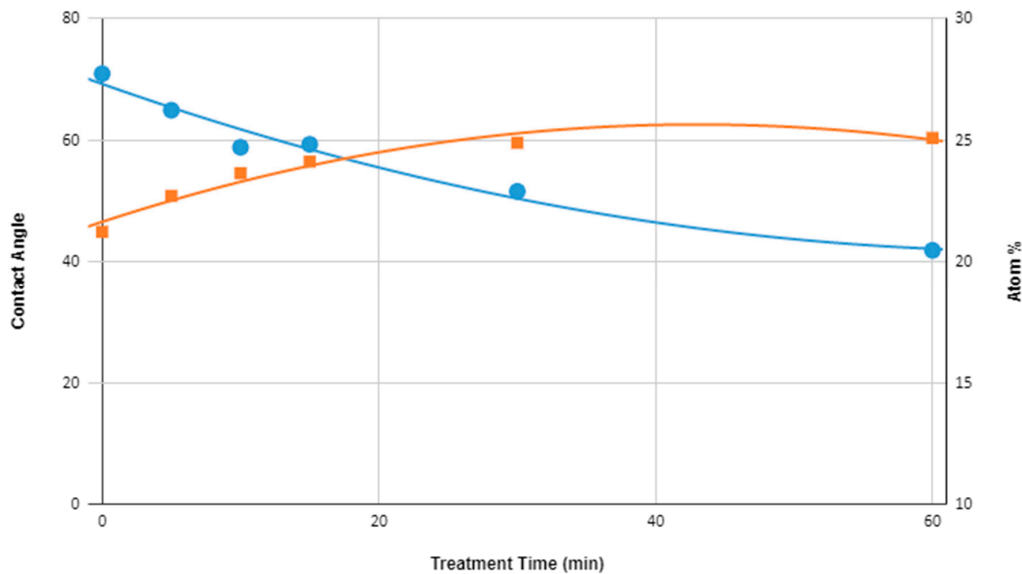


Figure 3. PES treated with VUV photo-oxidation showing an increase in atomic % of oxygen and a decrease in the water contact angle in degrees as a function of treatment time.

Washing the VUV photo-oxidized PES samples with water or ethanol increased the water contact angle from the average of 41.9° up to 66° for 60 min treatment.

3.2. XPS Chemical State Analysis

The overlapped C 1s spectra for the control and VUV photo-oxidized PES samples reported in Figure 2 are displayed in Figure 4. Curve fitting of the spectra (Table 1) showed a decrease in sp^2 C-C aromatic group bonding and an increase in C-O, C-S, and O=C-OH functional groups with treatment time.

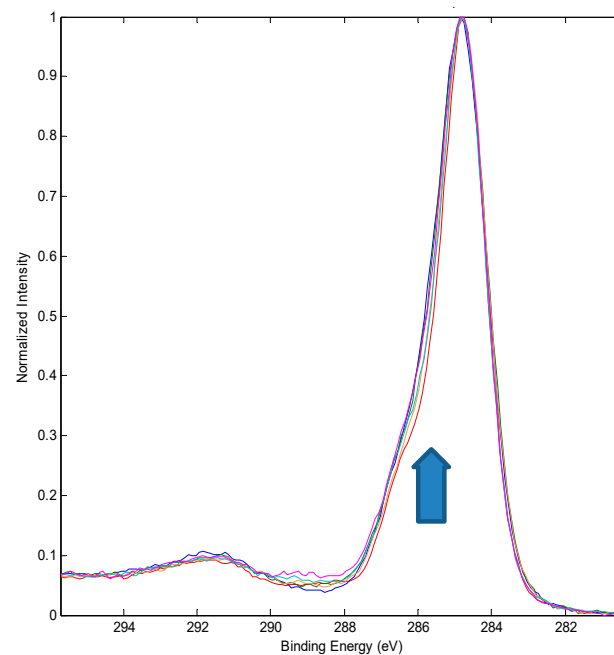


Figure 4. Overlapped C 1s spectra for control and PES samples treated with VUV photo-oxidation. The arrow indicates increasing treatment time for 0, 5, 10, 15, 30, and 60 min.

Table 1. Assignments [15] and % areas for the C 1s peaks in Figure 4 as determined by curve-fitting. Carbons (1), (2), and (3) are illustrated in Figure 1.

Binding Energy (eV)	Species	Treatment Time (min)					
		0	5	10	15	30	60
284.7	C-C aromatic ring (1)	65.0	63.0	63.3	64.0	62.7	62.5
285.3	C-S (2)	15.6	15.3	16.6	16.2	16.8	16.1
286.3	C-O (3), C-O (286.1)	15.0	16.8	16.7	16.1	16.5	17.1
287.0	C=O	0	0	0	0	0	0.1
288.6	O-C=O	0	0	0	0	0	0
289.1	O=C-OH	0	0	0	0	0.4	0.5
289.8	O-(C=O)-O	0	0	0	0	0	0
291.5	Energy loss peak	4.0	4.9	3.4	3.7	3.6	3.7

The changes in the O 1s spectra (Figure 5) confirmed the oxidation of the PES surface (Table 2).

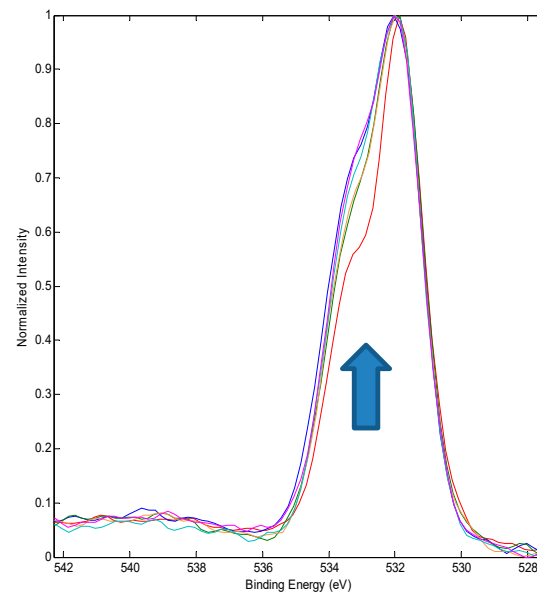


Figure 5. Overlapped O 1s spectra for control and PES samples treated with VUV photo-oxidation. The arrow indicates increasing treatment time for 0, 5, 10, 15, 30, and 60 min.

Table 2. Assignments [15] and % areas for O 1s peaks in Figure 5 as determined by curve-fitting for the oxygen atoms (1) and (2) in Figure 1. The * indicates the O atom assigned to that binding energy.

Binding Energy (eV)	Species	Treatment Time (min)					
		0	5	10	15	30	60
531.6	O=S (1)	69.4	45.8	47.3	47.2	46.2	44.3
532.2	O*=C-OH	0	19.0	18.3	17.8	19.5	19.9
533.3	C-O-C (ring) (2) (533.3), C-O (533.1) too close to separate, O-C-O*H (533.5)	30.6	35.2	34.4	35.0	34.4	35.8

Curve-fitting the S 2p spectra (Figure 6) gave the correct ratio of 2:1 for $2p^{3/2}$ and $2p^{1/2}$ species separated by 1.2 eV (Table 3) for untreated PES [15]. With treatment time, there is an increase in the formation of sulphonate ($-\text{SO}_3$) and sulphate ($-\text{SO}_4$) moieties (Table 3).

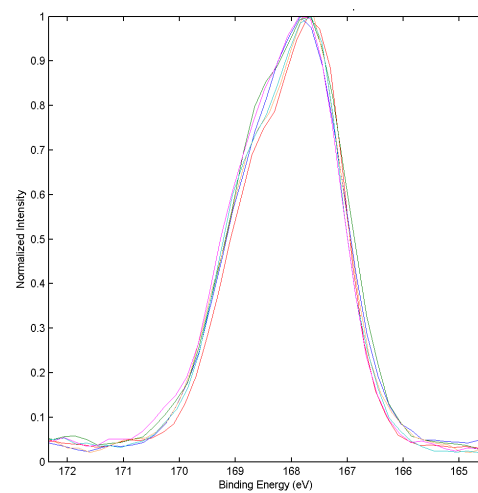


Figure 6. Overlapped S 2p spectra for control and PES samples treated with VUV photo-oxidation for 0, 5, 10, 15, 30, and 60 min. Due to the small changes in S chemical states (Table 3), an arrow indicating increasing treatment time was not possible in this Figure.

Table 3. Assignments [15] and % areas for S 2p^{3/2} and S 2p^{1/2} peaks as determined by curve-fitting the spectra in Figure 6.

Binding Energy (eV)	Species	Treatment Time (min)					
		0	5	10	15	30	60
167.6	C-S=O S 2p _{3/2}	66.1	65.6	65.8	66.7	64.8	63.5
168.8	C-S=O S 2p _{1/2}	33.9	31.8	30.9	31.1	32.3	33.5
168.6	Sulphonate or Sulphate S 2p _{3/2}	0	1.7	2.1	1.5	1.9	2.0
169.8	Sulphonate or Sulphate S 2p _{1/2}	0	0.9	1.2	0.7	1.0	1.0

3.3. Surface Topography for PES Treated with VUV Photo-Oxidation

The SEM results (Figures 7 and 8) showed no major changes in surface topography with treatment time consistent with previous VUV photo-oxidation studies of PS [9] and PBI [10].

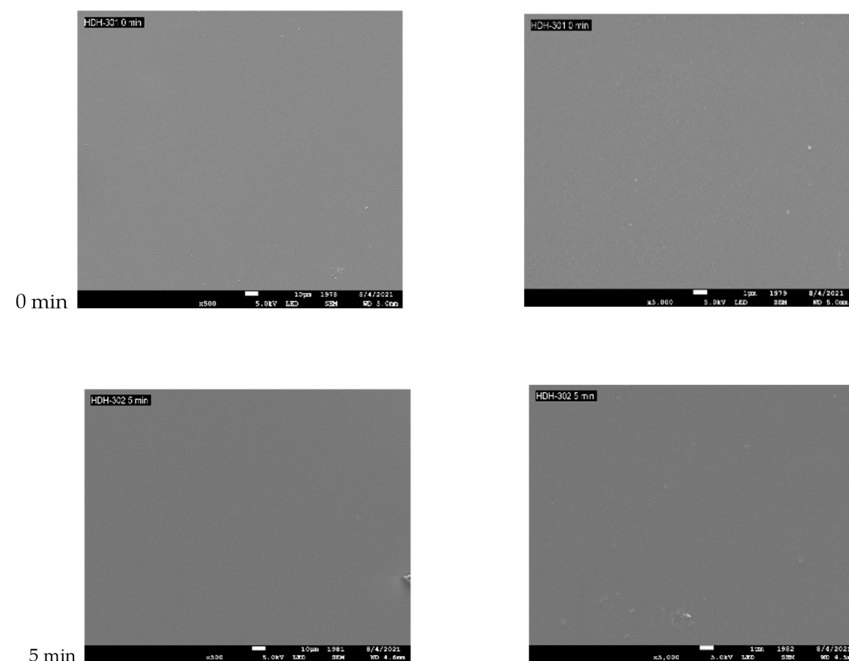


Figure 7. Cont.

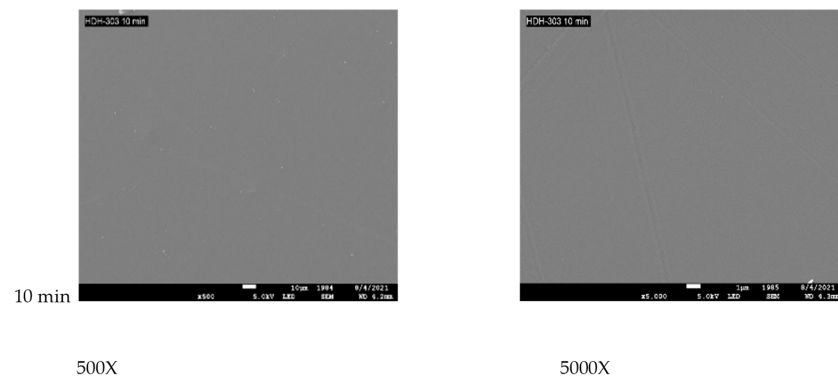


Figure 7. SEM surface topographic images at 500× and 5000× magnification after 0, 5, and 10 min treatment with VUV photo-oxidation.

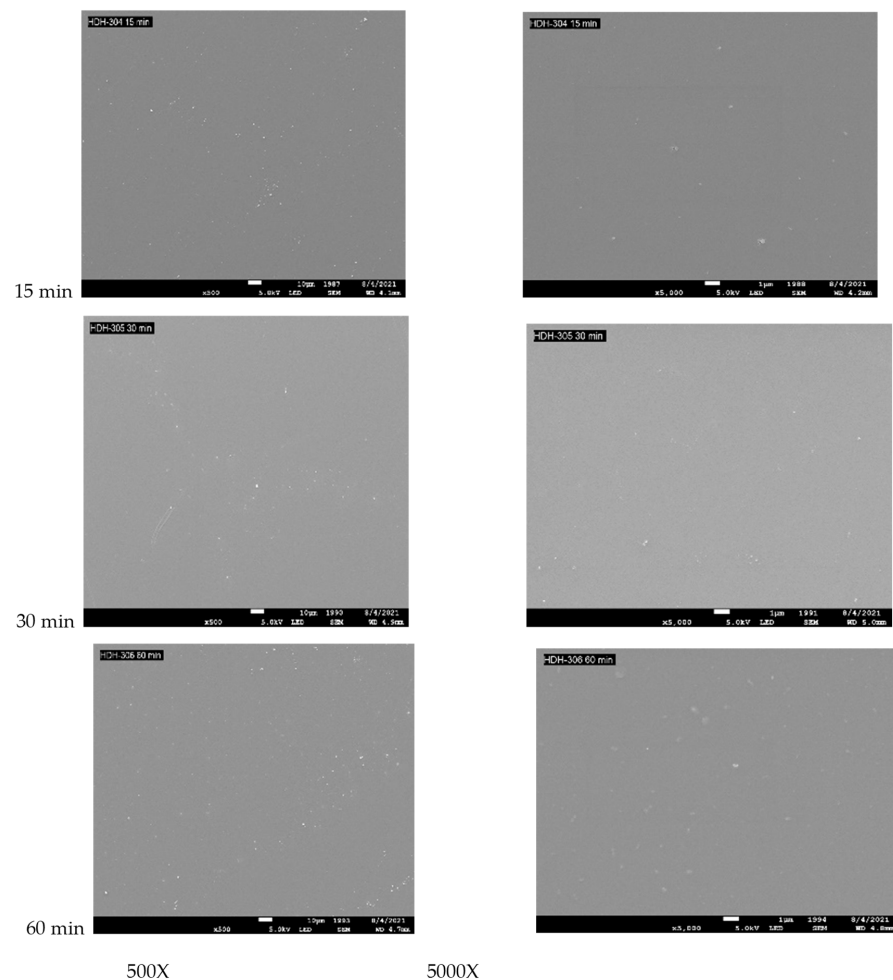
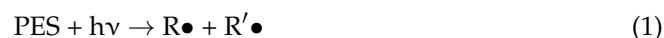


Figure 8. SEM surface topographic images at 500× and 5000× magnification after 15, 30, and 60 min treatment with VUV photo-oxidation.

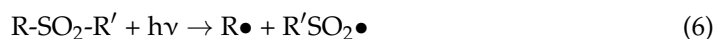
4. Discussion

Photochemical interactions contribute to the decrease in the aromatic carbon (C-C sp²) concentrations reported in Table 1. Photoabsorption of a number of ring substituted analogues of polystyrene (PS) occurs at ca. 270 nm and extends into the vacuum UV region [16–18]. As with PS, VUV photons absorbed by the aromatic functional groups in PES have a total energy content in excess of that required for bond scission producing free radicals on the surface by reaction (1) [9]. Reactions (2) to (5), involving the R• free radical,

illustrate the formation of the RO• free radical which, when added to the polymer, would contribute to the observed C-O moieties in this study (Table 1).



Similarly, the highly energetic 104.8 nm (272.7 kcal) and 106.7 nm (267.9 kcal) photons have sufficient energy to photo-dissociate the ether moiety in PES, as observed by UV photolysis of diphenyl ether ([13], pp. 447), and break the C-S bond which has a bond strength of ca. 103 kcal ([14], pp. 106) resulting in RO• radicals contributing to the observed C-O moieties (Table 1). Breakage of the C-S bond in PES by Equation (6) leads to the formation of the sulphonate (-SO₃) function group by Equation (7) or by reactions similar to Equations (2) and (5) involving R'SO₂• producing R'SO₃•.



Oxidation of the sulphonate group would lead to the formation of the sulphate compound, RO-SO₂-OR, by Equations (8) and (9) [19].



Additionally, photo-oxidation of the aromatic rings may form peroxy free radicals that abstract a hydrogen atom to produce reactive hydroperoxide groups, ROOH, resulting in the formation of hydroxylated-containing compounds, such as the carboxylic acid (Figure 5, Table 2) [20] and sulphonate/sulphate moieties (Figure 6, Table 3) observed in this study.

UV photo-oxidation of PES with 253.7 nm photons has been reported to cause cleavage of the aromatic rings and photo-dissociation of the C-S bond resulting in hydroxylated and carbonylated products with low molecular weight [21,22]. Carbon dioxide was also released during 253.7 nm photo-oxidation of PES [22] which is consistent with polymer chain bond breakage and the observations in this study of: (1) no detected carbonate/anhydride groups which would release CO₂; and (2) the washing away of a weak boundary layer (WBL) of oxidized material after treatment. The low penetration depth of VUV radiation contributes to bond breakage forming a WBL which was observed by washing the 60 min treated samples with water or ethanol resulting in an increase of water contact angle from the average of 41.9° up to 66°.

VUV photo-dissociation of oxygen may also assist in the surface modification in this study. The reaction of PES with O atoms generated downstream from the afterglow of a 200 W RF oxygen plasma showed an increase in wettability and the formation of O-C=O and C-O functional groups [23], consistent with a mechanism where O atoms insert into the aromatic double bond forming an epoxy ring which dissociates into carbonyl, aldehyde, and carboxylic acid functional groups observed with a remote He/O₂ atmospheric plasma [24]. The 26–34 W MW plasma and the oxygen concentration used in this study did not generate sufficient O atom concentration to produce significant amounts of the O-C=O and C-O functional groups (Figure 4, Table 1).

The negligible change of the S at% observed in this study is consistent with no gaseous SO₂ being released during photo-oxidation as reported during studies of PES photolyzed with 253.7/184.9 nm radiation [25,26].

The small increase in O concentration in this study (3.7 ± 1.0 at%) resulted in a 42% decrease in water contact angle (Figure 3) compared to 253.7/184.9 nm UV photo-oxidation (43%, 43%) [25], 253.7 nm UV photo-oxidation (47.5%, 45%) [25], and treatment with ozone in the absence of radiation (25%, 27%) [19].

VUV photolysis of PES in ambient oxygen-containing air with a Xenon excimer lamp, which emits photons at a wavelength of 172 nm, showed hemisphere-like structures on the surface that were washed away in polar solvents [27]. No significant changes in surface topography with VUV photo-oxidation treatment time was observed in this low pressure study. Using atmospheric air or oxygen, ozone is produced by Equation (10) involving a stabilizing molecule (M) such as nitrogen and/or oxygen.



The large amount of ozone formed in the 172 nm study may be very reactive with the PES surface causing the formation of the WBL affecting the surface roughness. When an electric generator was used to produce only an ozone concentration of ca. $6 \pm 2\%$ of the volume of oxygen, no significant changes in surface topography of PES were detected [19].

Previously, PES was surface treated with samples placed inside a Biopolar pulsed powered plasma of low pressure Ar and then oxidized when exposed to air leading to time dependent oxidation changes on the surface. Besides being exposed to VUV photons, the plasma consists of many excited particles (e.g., electrons, radicals, positively and negatively charged ions, etc.) which can modify the surface via a multitude of processes. Hydrophilic C-O groups were detected on the surface and surface roughness increased with treatment time [28].

Treatment of PES in Ar/O₂ plasma using an Oxford Instruments (Plasmalab80Plus) 200 W plasma generator showed an increase in hydrophilicity with small structural changes [29] while a 20 W RF oxygen-containing plasma had severe influence on surface topography [30]. Higher concentrations of oxygen in 50 W RF Ar/oxygen plasma and longer exposure times increased hydrophilicity and enhanced the opening of pores to improve permeability through the PES membrane [31].

5. Conclusions

XPS analysis of VUV photo-oxidized PES with 104.8 and 106.7 nm photons from a MW Ar plasma increased the O at% by 3.7 ± 1.0 at% up to a saturation level along with a decrease in sp² C-C aromatic group bonding, and an increase in C-O, C-S, O=C-OH, -SO₃ and -SO₄ functional groups. The water contact angle decreased from 71.9°, for untreated PES, down to a saturation level of 41.9° with treatment. Because SEM showed no significant changes in surface topography, the increase in hydrophilicity was mainly due to oxidation of the surface. Washing the saturated VUV photo-oxidized PES samples with water or ethanol increased the water contact angle up to 66° indicating the formation of a weak boundary layer.

Author Contributions: S.O., R.K. and H.H. performed the experiments. J.S. helped initiate the research. M.M. conducted the XPS analyses. T.A. and G.K.T. did surface topography analyses. G.A.T. supervised the students, designed the experiments, and wrote the bulk of the manuscript. All authors have read and agreed to the published version of the manuscript.

Funding: This research received no external funding.

Institutional Review Board Statement: Not applicable.

Informed Consent Statement: Not applicable.

Data Availability Statement: The data presented are available in this publication.

Conflicts of Interest: The authors declare no conflict of interest.

References

1. Miller, D.J.; Dreyer, D.R.; Bielawski, C.W.; Paul, D.R.; Freeman, B.D. Surface modification of water purification membranes. *Angew. Chem. Int. Ed.* **2017**, *56*, 4662–4711. [[CrossRef](#)] [[PubMed](#)]
2. Alenazi, N.A.; Hussein, M.A.; Alamry, K.A.; Asiri, A.M. Modified polyether-sulfone membrane: A mini review. *Des. Monomers Polym.* **2017**, *20*, 532–546. [[CrossRef](#)] [[PubMed](#)]
3. Zhao, C.; Xue, J.; Ran, F.; Sun, S. Modification of polyethersulfone membranes—A review of methods. *Prog. Mater. Sci.* **2013**, *58*, 76–150. [[CrossRef](#)]
4. Aguilar-Sanchez, A.; Jalvo, B.; Mautner, A.; Nameer, S.; Poehler, T.; Tammelin, T.; Mathew, A.P. Waterborne nanocellulose coatings for improving the antifouling and antibacterial properties of polyethersulfone membranes. *J. Membr. Sci.* **2021**, *620*, 118842–118851. [[CrossRef](#)]
5. Ahmad, M.W.; Dey, B.; Al Saidi, A.K.A.; Choudhury, A. Functionalized-graphene reinforced polyethersulfone nanocomposites with improved physical and mechanical properties. *Polym. Compos.* **2020**, *41*, 4104–4116. [[CrossRef](#)]
6. Suhartono, J.; Pertiwi, D.S.; Noersalim, C.; Yulianingsih, D.; Sofianti, F.; Saptorio, A.; Chafidz, A. Characteristics and performances of blended polyethersulfone and carbon-based nanomaterial membranes: Effect of nanomaterial types and air exposure. *Chem. Eng. Technol.* **2020**, *43*, 1630–1637. [[CrossRef](#)]
7. Takacs, G.A.; Miri, M.J.; Kovach, T. Vacuum UV surface photo-oxidation of polymeric and other materials for improving adhesion: A critical review. *Rev. Adhes. Adhes.* **2020**, *8*, 555–581.
8. Samson, J.A.R. *Techniques of Vacuum Ultraviolet Spectroscopy*; John Wiley & Sons: New York, NY, USA, 1967.
9. Li, X.; Toro, M.; Lu, F.; On, J.; Bailey, A.; Debies, T.; Mehan, M.; Gupta, S.K.; Takacs, G.A. Vacuum UV photo-oxidation of polystyrene. *J. Adhes. Sci. Technol.* **2016**, *30*, 2212–2223. [[CrossRef](#)]
10. Kovach, T.; Boyd, S.; Garcia, A.; Fleischer, A.; Vega, K.; Hilfiker, R.; Shertok, J.; Mehan, M.; Gupta, S.K.; Takacs, G.A. Surface modification of polybenzimidazole (PBI) with microwave generated vacuum ultraviolet (VUV) photo-oxidation. *Curr. Microv. Chem.* **2021**, *8*. [[CrossRef](#)]
11. Badey, P.; Urbaczewski-Espunche, E.; Jugnet, Y.; Sage, D.; Minh Duc, T.; Chabert, B. Surface modification of poly(tetrafluoroethylene) by microwave plasma downstream treatment. *Polymer* **1994**, *35*, 2472–2479. [[CrossRef](#)]
12. Lens, J.P.; Spaay, B.; Terlingen, J.G.A.; Engbers, G.H.M.; Feijen, J. Mechanism of the immobilization of surfactants on polymer surfaces by means of an argon plasma treatment: Influence of UV radiation. *Plasmas Polym.* **1999**, *4*, 159–182. [[CrossRef](#)]
13. Calvert, J.G.; Pitts, J.N. *Photochemistry*; John Wiley & Sons: New York, NY, USA, 1966; pp. 206–447.
14. Okabe, H. *Photochemistry of Small Molecules*; John Wiley & Sons: New York, NY, USA, 1978; pp. 106–179.
15. Beamson, G.; Briggs, D. *High Resolution XPS of Organic Polymers*; John Wiley & Sons: Chichester, UK, 1991.
16. Weir, N.A. Photo and photooxidation reactions of polystyrene and of ring substituted polystyrenes. *Dev. Polym. Degrad.* **1982**, *4*, 143–188.
17. Geuskens, G.; Baeyens-Volant, D.; Delaunois, G.; Lu-Vinh, Q.; Piret, W.; David, C. Photo-oxidation of polymers I. A quantitative study of the chemical reactions resulting from irradiation of polystyrene at 253.7 nm in the presence of oxygen. *Euro. Polym. J.* **1978**, *14*, 291–297. [[CrossRef](#)]
18. Partridge, R.H. Vacuum-ultraviolet absorption spectrum of polystyrene. *J. Chem. Phys.* **1967**, *47*, 4223–4227. [[CrossRef](#)]
19. Lutondo, S.; Turo, M.; Sachdev, S.; Shertok, J.; Bailey, A.; Mehan, M.; Gupta, S.K.; Takacs, G.A. Surface modification of polyethersulfone (PES) with ozone. *Ozone Sci. Eng.* **2019**, *41*, 448–453. [[CrossRef](#)]
20. Munro, H.S.; Clark, D.T. An ESCA investigation of the surface photo-oxidation of polyethersulphone. *Polym. Degrad. Stab.* **1985**, *1*, 225–231. [[CrossRef](#)]
21. Kilduff, J.E.; Mattaraj, S.; Pieracci, J.P.; Belfort, G. Photochemical modification of poly(ethersulfone) and sulfonated poly(sulfone) nanofiltration membranes for control of fouling by natural organic matter. *Desalination* **2000**, *132*, 133–142. [[CrossRef](#)]
22. Rivaton, A.; Gardette, J.L. Photodegradation of polyethersulfone and polysulfone. *Polym. Degrad. Stab.* **1999**, *66*, 385–403. [[CrossRef](#)]
23. Vrlinic, T.; Vesel, A.; Cvelbar, U.; Krajnc, M.; Mozetic, M. Rapid surface functionalization of poly(ethersulphone) foils using a highly reactive oxygen-plasma treatment. *Surf. Interface Anal.* **2007**, *39*, 476–481. [[CrossRef](#)]
24. Gonzalez, E.; Barankin, M.D.; Guschl, P.C.; Hicks, R.F. Ring opening of aromatic polymers by remote atmospheric-pressure plasma. *IEEE Trans. Plasma Sci.* **2009**, *37*, 823–831. [[CrossRef](#)]
25. Cisse, I.; Oakes, S.; Sachdev, S.; Toro, M.; Lutondo, S.; Shedden, D.; Atkinson, K.M.; Shertok, J.; Mehan, M.; Gupta, S.K.; et al. Surface modification of polyethersulfone (PES) with UV photo-oxidation. *Technologies* **2021**, *9*, 36. [[CrossRef](#)]
26. Norrman, K.; Kingshott, P.; Kaeselev, B.; Ghanbari-Siahkali, A. Photodegradation of poly(ether sulfone) Part 1. A time-of-flight secondary ion mass spectrometry study. *Surf. Interface Sci.* **2004**, *36*, 1533–1541.
27. Arikan, E.; Holtmannspotter, J.; Zimmer, F.; Hofmann, T. The role of chemical surface modification for structural adhesive bonding on polymers—Washability of chemical functionalization without reducing adhesion. *Int. J. Adhes. Adhes.* **2019**, *95*, 102409–102420. [[CrossRef](#)]
28. Singh, N.L.; Pelagade, S.M.; Rane, R.S.; Mulkherjee, S.; Deshpande, U.P.; Ganeshan, V.; Shripathi, T. Influence of argon plasma treatment on polyethersulphone surface. *Pramana* **2013**, *80*, 133141. [[CrossRef](#)]

29. Michaljanicova, I.; Sleepicka, P.; Vesely, M.; Svorcik, V. Efficient nanostructure construction of polymer substrates by plasma treatment for tissue engineering. In Proceedings of the 2016 IEEE 16th International Conference on Nanotechnology (IEEE-NANO), Sendai, Japan, 22–25 August 2016; pp. 149–152.
30. Hopkins, J.; Badyal, J.P.S. Plasma modification of poly(ether sulfone). *Macromolecules* **1994**, *27*, 5498–5503. [[CrossRef](#)]
31. Saxena, N.; Prabhavathy, C.; Sirshendu, D.; DasGupta, S. Flux enhancement by argon-oxygen plasma treatment of polyethersulfone membranes. *Sep. Purif. Technol.* **2009**, *70*, 160–165. [[CrossRef](#)]